Physical and dynamical characterization of hyperbolic comet C/2017 U7 (PANSTARRS)

M. Evangelista-Santana[a] (Researcher), J. M. Carvano[a] (Researcher), M. De Prá[b] (Researcher), R. de la Fuente Marcos[c] (Researcher), C. Schambeau[b] (Researcher), J. Licandro[d,e] (Researcher), C. de la Fuente Marcos[f] (Researcher), A. C. Souza-Feliciano[a] (Researcher) and N. Pinilla-Alonso[b] (Researcher)

[a] *Observatório Nacional, rua Gal. José Cristino 77, CEP 20921-400, Rio de Janeiro, Brazil*
[b] *Florida Space Institute, University of Central Florida, Orlando, EUA*
[c] *AEGORA Research Group, Facultad de Ciencias Matemáticas, Universidad Complutense de Madrid, Ciudad Universitaria, 28040, Madrid, Spain*
[d] *Instituto de Astrofísica de Canarias, Tenerife, Spain*
[e] *Universidad de La Laguna, La Laguna, Spain*
[f] *Universidad Complutense de Madrid, Ciudad Universitaria, 28040, Madrid, Spain*

ARTICLE INFO

Keywords:
comets, photometry, spectroscopy, dynamics

ABSTRACT

We present here a dynamical and observational study of the comet C/2017 U7 (PANSTARRS). This comet was discovered in 2017 and found to have a hyperbolic orbit. Our dynamical analysis shows that the object has probably originated in the Oort cloud, however an interstellar origin can not be discarded. The observations were obtained in 2018 and 2019 using the Goodman High Throughput Spectrograph (GHTS) at the SOAR telescope. We obtained visible spectra covering the wavelength range of $0.5 - 0.9\mu$m and also images in the SDSS filters system. Both the low-resolution reflectance spectrum and the reflectance spectra derived from the SDSS filters show an atypical band at $\sim 0.595\mu$m. We conducted a comparative study of the colors and reflectance spectra of different small body populations (e.g., comets, Centaurs, and trans-Neptunian objects *or TNOs*) from the literature and concluded that the spectra and the colors of this comet are atypical, showing only some overlap with those of some known members of the TNOs and Centaurs, within the large uncertainties of the measurements of *those populations*. It is found that the feature and overall spectral shape can be reproduced by laboratory spectra of kerite, a template for aliphatic-rich hydrocarbons that has been previously identified in NIR cometary spectra absorptions. It is tentatively proposed that the unusual spectral shape is the result of a particle size distribution of dust grains in the coma or on the surface that has arisen due to a low grain ejection velocity from the surface and large nucleus size.

1. Introduction

The small bodies of the solar system can be considered the most pristine objects in our planetary system. Specifically, comets are believed to hold volatile content and are capable of providing information about the protoplanetary disk formation and evolution (Bauer et al., 2017; Hui, 2018).

It is generally assumed that comets have sources in the trans-Neptunian belt (short-period comets) and the Oort cloud (long-period comets), see Jewitt (2015). Many of these comets can enter the inner solar system, but in some cases they show high perihelion distances, q. Some even follow weakly hyperbolic

marcalsantana@on.br (M. Evangelista-Santana); carvano@on.br (J.M. Carvano); mariondepra@gmail.com (M. De Prá)
ORCID(s): 0000-0003-0670-639X (J.M. Carvano)

trajectories. Although the mechanism of activation is fairly well understood for the comets that have closer approaches to the Sun, there is a gap of knowledge regarding the objects with high perihelion distance (q >5 au). Activity in this region is most likely mainly driven by crystallization of amorphous ice and/or sublimation of hyper volatile species (Everhart, 1982; Weissman, 1982; Fernández et al., 2004).

This scenario reflects a possible bias in the sample of observed comets, where most of the *well-studied* objects are Jupiter-Family comets (JFCs), originating at the trans-Neptunian belt, and few are long-period comets, originating at the Oort cloud. To overcome this bias and to more thoroughly understand the current structure of the solar system, and how it formed and evolved, it is critical to characterize the compositions, activity mechanisms and other physical properties among the different comet populations.

In particular, the Oort cloud is a spherically distributed reservoir of small icy bodies that, according to indirect observational evidence, surrounds the outskirts of the solar system and may have formed nearly 4.6 Gyr ago. Studies of objects that have a probable origin in this region have revealed a heterogeneous nature (e.g., Oort, 1950; Stern and Weissman, 2001; Fernández et al., 2004; Meech et al., 2016) and suggest that part of the material in the Oort cloud could have an extrasolar origin, containing materials captured from the protoplanetary discs of other stars while still forming within its nascent star cluster *(see for example Portegies Zwart et al. 2021)*. However, little is still known about the existence, extent and dominant physical properties of objects from this region.

In this context, A/2017 U7 was discovered on October 29, 2017, when it was at 7.8 au from the Sun and moving towards perihelion at 6.4 au, by the 1.8 m Pan-STARRS 1 Ritchey-Chretien telescope at Haleakala (Bressi et al., 2018) observing for the Panoramic Survey Telescope and Rapid Response System (Pan-STARRS, Kaiser 2004; Denneau et al. 2013). The object was initially regarded as asteroidal, A/2017 U7, *therefore the initial prefix A/*, but it was eventually confirmed to be a comet, C/2017 U7 (PANSTARRS) (Bressi et al., 2020).[1] Initial orbit determinations placed this object among the group of hyperbolic asteroids (orbital eccentricity, $e > 1$) and later among the hyperbolic comets. The solution available on March 4, 2018, when the discovery was announced, gave a value of the heliocentric eccentricity of 1.00176±0.00012. A recent orbit determination (see Table 1), gives *1.000991±0.000009* that is a moderate value of e among those of known hyperbolic comets; the orbit determination in Table 1 is based on *816* observations for a data-arc of *1421* days. A/2017 U7 was first observed only 10 days after the discovery of 1I/2017 U1 ('Oumuamua), the first known interstellar object (see for example the review in Hainaut et al. 2018). When first announced, A/2017 U7 was regarded as a candidate for being an interstellar object, albeit with very low hyperbolic excess velocity with respect to the barycenter of the solar system. This was our initial motivation

[1] https://www.minorplanetcenter.net/mpec/K20/K20F58.html

for studying C/2017 U7 (PANSTARRS).

We present here a study of the spectroscopic, photometric and dynamical properties of the hyperbolic comet C/2017 U7 (PANSTARRS). An exploration of the orbital evolution of the object is shown in section 2. The observations and reduction techniques are described in section 3, and the analysis of the observational data is presented in section 4. Finally, we present a discussion of these results and draw our conclusions in section 5.

2. Comet C/2017 U7 (PANSTARRS): past, present and future dynamical evolution

In order to study the dynamical evolution of C/2017 U7 (PANSTARRS), we use data —heliocentric and barycentric orbital elements and their uncertainties, *common for both*— provided by Jet Propulsion Laboratory's Solar System Dynamics Group Small-Body Database (JPL's SSDG SBDB, Giorgini 2015)[2] *and based on JPL's Planetary and Lunar Ephemerides DE440 and DE441 (Park et al., 2021),* and full N-body calculations carried out with software written by Aarseth (2003)[3] that implements the Hermite integration scheme described by Makino (1991). These numerical simulations do not include non-gravitational forces; the physical model and additional details are described in de la Fuente Marcos and de la Fuente Marcos (2012). *The effects of Galactic tides and stellar perturbations on the calculations as discussed by Królikowska and Dybczyński (2018) have been neglected as they appear to be relatively unimportant for short integrations like ours —compare the results for C/2017 K2 (PANSTARRS) in Królikowska and Dybczyński (2018) and de la Fuente Marcos and de la Fuente Marcos (2018). Such effects cannot be ignored when much longer integrations are attempted as the orbital period of the solar system around the center of the Galaxy is close to 250 Myr (our longest integrations span just 6 Myr).* Cartesian state vectors were obtained from JPL's HORIZONS[4] *(also based on DE440/DE441)* or computed using the Monte Carlo Covariance Matrix (MCCM) method described by de la Fuente Marcos and de la Fuente Marcos (2015) with covariance matrices obtained from HORIZONS that is also the source of other input data necessary to carry out the calculations such as barycentric Cartesian state vectors for planets and other bodies. The approach applied here has been previously used in de la Fuente Marcos and de la Fuente Marcos (2018, 2019), Licandro et al. (2019), de la Fuente Marcos et al. (2019), and de León et al. (2020).

[2] https://ssd.jpl.nasa.gov/sbdb.cgi
[3] http://www.ast.cam.ac.uk/~sverre/web/pages/nbody.htm
[4] https://ssd.jpl.nasa.gov/?horizons

Table 1
Heliocentric and barycentric orbital elements and 1σ uncertainties of C/2017 U7 (PANSTARRS). The orbit determination has been computed at epoch JD *2458777.5* that corresponds to 00:00:00.000 TDB, Barycentric Dynamical Time, on *2019 October 21*, J2000.0 ecliptic and equinox. Source: JPL's SSDG SBDB (solution date, *2021-Jul-26 23:12:24* PDT).

Orbital parameter		Heliocentric	Barycentric
Perihelion distance, q (au)	=	*6.417304±0.000008*	*6.409861*
Eccentricity, e	=	*1.000991±0.000009*	*0.998413*
Inclination, i (^{0})	=	*142.63527±0.00002*	*142.65424*
Longitude of the ascending node, Ω (^{0})	=	*276.23233±0.00002*	*276.18950*
Argument of perihelion, ω (^{0})	=	*326.04347±0.00008*	*326.06799*
Mean anomaly, M (^{0})	=	*0.0000749±0.0000010*	*0.0001483*
Absolute magnitude, H (mag)	=	8.8±0.9	

Table 2
Barycentric Cartesian state vector of C/2017 U7 (PANSTARRS): components and associated 1σ uncertainties. *Epoch 2458777.5 TDB (2019-Oct-21.0)*. Source: JPL's SBDB.

Component		value±1σ uncertainty
X (au)	=	$3.177654393232998\times10^{+0}\pm4.01804054\times10^{-6}$
Y (au)	=	$-5.208536696177243\times10^{+0}\pm6.01295174\times10^{-6}$
Z (au)	=	$-1.982092111114977\times10^{+0}\pm2.86906024\times10^{-6}$
V_X (au d^{-1})	=	$-5.867065291363123\times10^{-3}\pm9.28855347\times10^{-9}$
V_Y (au d^{-1})	=	$-5.796459892690215\times10^{-3}\pm1.00112837\times10^{-8}$
V_Z (au d^{-1})	=	$4.927699142603646\times10^{-3}\pm8.98470643\times10^{-9}$

2.1. Current orbital status

Although the heliocentric orbit determination in Table 1 is hyperbolic at the *117σ* level, the barycentric one is not hyperbolic at the *187σ* level. Therefore, C/2017 U7 (PANSTARRS) is at the moment gravitationally bound to the solar system, even if weakly. On the other hand, on May 18, 2020, C/2017 U7 (PANSTARRS) experienced a close approach to Jupiter at about 1.66 au from its center. This flyby took place at a relative velocity *close to* 28 km s^{-1}, which is relatively *slow* so its long-term dynamical effects might not have been negligible. Long-term calculations (see below) may show the true effects of such an encounter. *Figure 1 shows that the evolution of representative control orbits with Cartesian vectors separated ±3σ and ±9σ from the nominal values in Table 2 is virtually identical in the neighborhood of the zero time instant. The figure reveals that the short-term evolution of C/2017 U7 (PANSTARRS) is very stable and any orbit determination compatible with the available data produces nearly the same results in the time interval (−0.25, +0.25) Myr.*

2.2. Past orbital evolution

In order to investigate the orbital evolution of C/2017 U7 (PANSTARRS) over the past few Myr, we have *performed calculations in the time interval (−3, +3) Myr*. Our results are shown in Fig. 1 and they picture a

rather chaotic orbital evolution into the past. Close encounters with Jupiter make the reconstruction of the dynamical past of this comet difficult when considering times older than about 700 kyr and a probabilistic approach should be applied in order to arrive at reliable conclusions. At least *two* of the relevant orbits (*-3σ, in cyan, and $+9\sigma$, in red*) may lead to an ejection or, more properly, to a capture from interstellar space as we are considering an integration backwards in time. Such an evolution may be compatible with an origin in the Oort cloud as discussed by de la Fuente Marcos et al. (2018).

In order to understand better its possible origin, we have performed integrations backwards in time using MCCM to generate control orbits and find that the probability of this comet having been captured from interstellar space during the last *3 Myr is 0.11±0.05 (average and standard deviation of 10^3 experiments)*. Figure 2 shows results from these simulations. Most control orbits lead to barycentric distances with values below the aphelion distance that defines the domain of dynamically old Oort cloud comets (see Królikowska and Dybczyński 2017) as seen in the left panel. The most straightforward interpretation of these results is that C/2017 U7 (PANSTARRS) almost certainly did not arrive from interstellar space: It is a dynamically old object instead, with a likely origin in the solar system. This conclusion was also found by Hui (2018), using one of the earliest orbit determinations of C/2017 U7 (PANSTARRS), the solution available on March 4, 2018 pointed out above.

2.3. Future orbital evolution

Although the likely past orbital evolution of C/2017 U7 (PANSTARRS) as characterized by Figs. 1 and 2 was rather chaotic, the future orbital evolution is far more predictable. After the flyby with Jupiter on May 18, 2020, the comet seems to have received just enough impulse to leave the solar system. All the control orbits appear to lead to the same outcome (see Fig. 1). Our integrations shown in Fig. 2, right panel, indicate that its probability of escaping the solar system during the next *3 Myr is 0.75±0.05* and this value is likely to increase if we consider longer calculations. Its future evolution is similar to the one of C/2018 V1 (Machholz-Fujikawa-Iwamoto) as described by de la Fuente Marcos and de la Fuente Marcos (2019), *as both objects appear to be leaving the solar system*. Numerical simulations carried out by Hui (2018) with an orbit determination based on 87 observations spanning a data-arc of 176 days, indicated that this comet has a 60% chance of escaping the solar system during the next 1.5 Myr after its perihelion passage. This result is consistent with our own findings based on an improved orbit determination.

Comets that eventually leave the solar system as a result of close encounters with Jupiter are not uncommon. Comet C/1980 E1 (Bowell), with a current value of the heliocentric orbital eccentricity of *1.057733±0.000008* and a barycentric one of *1.047673*, is currently listed as the *sixth most hyperbolic object*

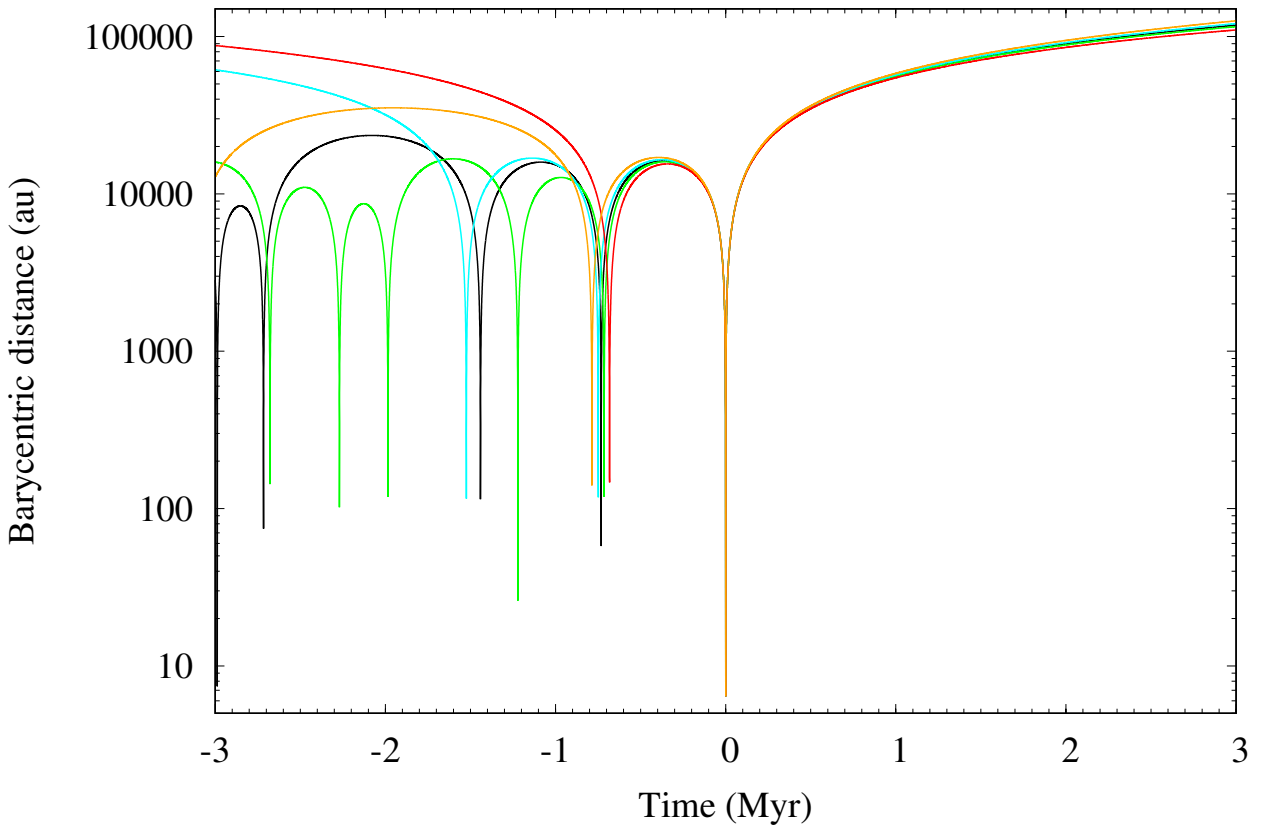

Figure 1: Evolution of the barycentric distance to the comet C/2017 U7 (PANSTARRS) as computed from the orbit determination in Table 1 (nominal in black) and relevant control orbits with Cartesian vectors separated $+3\sigma$ (in green), -3σ (in cyan), $+9\sigma$ (in red), and -9σ (in orange) from the nominal values in Table 2. *The output time-step size is 300 yr.* The zero time instant corresponds to epoch JD *2458777.5* TDB.

known —after 2I/Borisov with e=3.3562, 'Oumuamua with 1.2011, C/1893 N1 (Rordame-Quenisset) with 1.0823, C/2021 R2 (PANSTARRS) with 1.0771, and C/1954 O1 (Vozarova) with 1.0737, although the last three have few observations spanning short arcs— and its current path was the result of a close encounter with Jupiter on December 9, 1980 (see for example Buffoni et al. 1982; Branham 2013).

3. Observations and Data Reduction

We used the 4.1 m SOAR telescope at Cerro Pachón (Chile) to observe C/2017 U7 (PANSTARRS) on two nights: August 13th, 2018 and September 18th, 2019. On the first night, we used the Goodman High Throughput Spectrograph (GHTS) to acquire the object's visible spectrum and images. The spectrum was acquired using the GHTS Red Camera, with the grating of 400 l/mm (mode M2) and the 1.5" slit with no binning positioned along parallatic angle. This setup provided the visible spectra of the comet covering the wavelength range of 0.5-0.9 μm. The same setup was used to acquire the spectra of solar analog stars at an air mass similar to that of the object's observation. On the second night, we used the GHTS Red camera

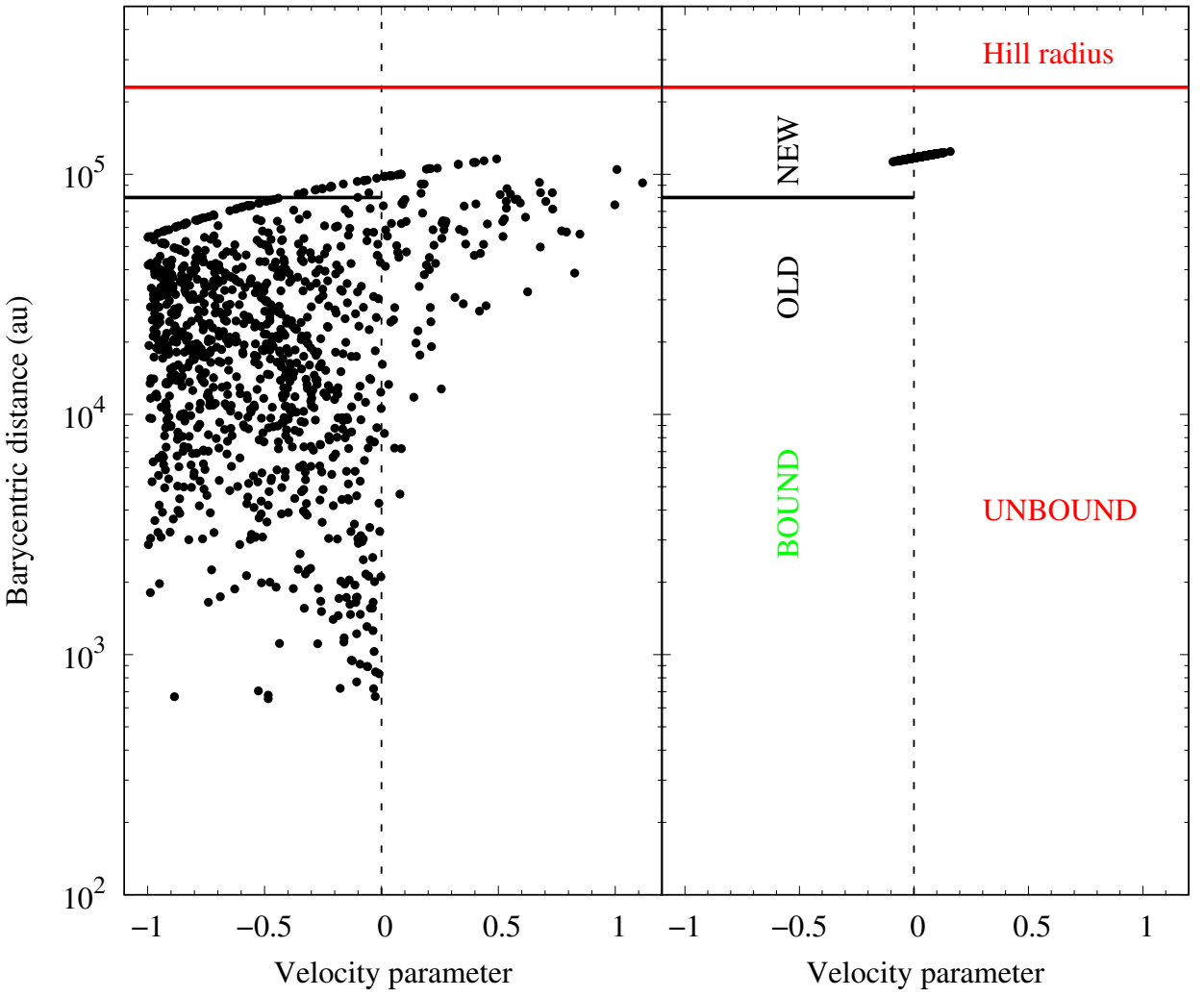

Figure 2: Values of the barycentric distance as a function of the velocity parameter *3 Myr* into the past (left panel) and future (right panel) for 1000 control orbits of C/2017 U7 (PANSTARRS) generated using the MCCM approach. The velocity parameter is the difference between the barycentric and escape velocities at the computed barycentric distance in units of the escape velocity. Positive values of the velocity parameter are associated with control orbits that could be the result of capture (left panel) or lead to escape (right panel). The thick black line corresponds to the aphelion distance —$a\ (1+e)$, limiting case $e = 1$— that defines the domain of dynamically old comets with $a^{-1} > 2.5 \times 10^{-5}$ au^{-1} (see Królikowska and Dybczyński 2017); the thick red line signals the radius of the Hill sphere of the solar system (see for instance Chebotarev 1965).

in imaging mode with the g-, r- , i-, and z-band filters in the Sloan Digital Sky Survey (SDSS) system. We used a 1 x 1 bin mode, the effective circular field of view was 7.2 arcmin (diameter) and the image scale was 0.15 arcsec pixel^{-1}. All observing circumstances surrounding the observations *carried* out with the SOAR telescope are shown in Table 3, and Table 4 lists the solar analogs used in the reduction of the spectroscopic observations.

C/2017 U7 (PANSTARRS) was also serendipitously observed by the Dark Energy Survey (Flaugher

et al., 2015) seven times on five nights between October 2017 and October 2018. These observations were made using the 4 m Victor M. Blanco at the Cerro Tololo Inter-American Observatory (CTIO) and the Dark Energy Camera (DECam) that has a field of view of diameter 2.2° with filters in the SDSS system. The observing circumstances are shown in Table 5. These retrieved archive DES images had been previously corrected using bias and master dome flats.

Table 3
All observations obtained with SOAR of comet C/2017 U7 (PANSTARRS). Δ : geocentric distance, r: heliocentric distance, and α: phase angle.

UT time	Airmass	Data type	Filter/spectral range (μm)	Exp. time (s)	$\Delta(au)$	$r(au)$	α
2018-08-13T02:57	1.67	Spectrum	0.5-0.9	3×600	6.162	6.943	5.6
2019-09-19T00:38	1.03	Image	g-band	4×300	5.888	6.417	8.0
2019-09-19T00:20	1.04	Image	r-band	4×150	5.888	6.417	8.0
2019-09-19T01:16	1.02	Image	i-band	4×150	5.888	6.417	8.0
2019-09-19T01:33	1.03	Image	z-band	4×150	5.888	6.417	8.0

Table 4
Solar analogs - Observing circumstances on 2018-08-13

Star	UT time	Airmass	Exp. time (s)
Landolt 107-998	23:05:59	1.16	3×90
Landolt 107-998	01:19:22	1.44	3×90
Landolt 107-684	23:18:56	1.16	3×90
Landolt 110-361	23:37:57	1.44	3×120
Landolt 110-361	01:46:30	1.14	3×120

Table 5
All observations obtained of DES for comet C/2017 U7 (PANSTARRS). Δ : geocentric distance, r: heliocentric distance, and α: phase angle.

UT time	Airmass	Data type	Filter/spectral range (μm)	Exp. time (s)	$\Delta(au)$	$r(au)$	α
2017-10-18T05:25	1.06	Image	g-band	1×90	7.217	7.902	5.5
2017-10-19T05:35	1.08	Image	g-band	1×90	7.220	7.898	5.5
2017-10-30T04:11	1.04	Image	i-band	1×90	7.274	7.857	6.1
2017-10-30T04:13	1.05	Image	z-band	1×90	7.274	7.857	6.1
2017-11-10T02:11	1.01	Image	r-band	1×90	7.356	7.816	6.6
2017-11-10T02:13	1.01	Image	g-band	1×90	7.356	7.816	6.6
2018-09-15T06:02	1.10	Image	r-band	1×90	6.094	6.862	5.7

The spectroscopic and imaging data were reduced using the Image Reduction and Analysis Facility (IRAF)[5]. The GHTS spectral images were first corrected for bias and then divided by a normalized flat field image. In sequence, we extracted the 2D spectra of C/2017 U7 (PANSTARRS) and those of the solar analogs

[5]IRAF is distributed by the National Optical Astronomy Observatories, which are operated by the Association of Universities for Research in Astronomy, Inc., under cooperative agreement with the National Science Foundation.

using the IRAF *APALL* task, centering the comet optocenter at the middle of the aperture. The background sky was measured (and subsequently subtracted) in a region close to the comet, free of coma, tail, and/or background stars. The final spectra was obtained by averaging the individual spectra of each target and calibrating the wavelength using HgArNe lamps. We divided the object's spectrum by each solar analogs spectra observed in the same night. This procedure allows for the investigation of possible systematic errors and also estimates of the uncertainty in the spectral slope. Finally, the spectra of C/2017 U7 (PANSTARRS) was produced by averaging all the object's spectra that had been divided the solar analog spectrum.

For all imaging data of C/2017 U7 (PANSTARRS), we applied an aperture photometry technique with radii varying between 1 and 50 pixels, using the task DIGIPHOT from the APPHOT package included in IRAF. However, in this particular case, specifically for active comets is necessary to consider the effects caused by seeing variations during each night, mainly for small apertures (Licandro et al., 2000). For each imaging sequence, the images were convolved with synthetic profiles in order to downgrade the seeing of each so as to match the worst seeing in each sequence (Licandro et al., 2000). Aperture photometry was then performed using radii between 1 and 50 pixels. Also, we used isolated stars for photometric calibrations that allowed for the use of larger apertures which minimized the effects of seeing variability. Photometric calibration for the SOAR observations on 2019-11-19 and for the DES observations were obtained by searching field stars with calibrated magnitudes listed in the SkyMapper Southern Sky Survey (Keller et al., 2007), using curve of growth (Howell, 1990) to determine the appropriate aperture.

4. Analysis and Results

4.1. Evolution of the coma

In order to measure the evolution of the coma within the time range of the observations gathered in this work, we initially performed a direct comparison of the radial profile of the comet with the profiles of field stars (Luu and Jewitt, 1992; Martino et al., 2019; De Prá et al., 2020), using three image sets: the DES images on 2017-10-18 and 2017-10-19 (g filter), the DES image on 2018-09-15 (r filter) *with scale of* 0.263 *arcsec pixel*$^{-1}$ and the 4 SOAR images on 2019-09-19 (r filter) *with scale of* 0.15 *arcsec pixel*$^{-1}$. The radial profiles of the comet and those of the stars were obtained using the PRADPROF task of the IRAF package. The radial profiles displayed in Figure 3 show the temporal evolution of the coma. The images that were obtained by DES in October 2017 show a radial profile with no detected coma *, although our data are not conclusive about the non-existence of activity at that time*. On the images obtained by DES in September 2018 and SOAR in September 2019, on the other hand, the distinction between the profile of the stars and that of the comet can be clearly seen. Therefore, the DES observations in October 2017 can be used to

characterize the nucleus if it is assumed that all flux received is from a bare nucleus.

In order to estimate the diameter of C/2017 U7's nucleus we first derived the absolute nuclear magnitude using the DES observations of 2017-11-10 in the g and r bands. From these observations, we calculated the V band magnitude through the relations given by Jurić et al. (2002). We assumed a constant value for the linear phase coefficient $\beta = 0.11$ mag deg^{-1} (Alvarez-Candal et al., 2016), obtaining a value for the absolute magnitude of the nucleus of $H = 10.87 \pm 0.06$ mag. Using albedos in the range 0.02–0.06, we obtained a diameter between 64 km and 37 km, and for an albedo of 0.04, typical of a comet nucleus, (Fernández et al., 2013) we obtained a diameter of ~ 45 km.

The evolution of the dust production rate of the comet was estimated using the $Af\rho$ parameter. This parameter was initialy defined by A'Hearn et al. (1984) on observations of the comet Bowell. As a general rule, it is assumed that larger A$f\rho$ values indicate higher dust production rates. Also, this parameter would be independent of the size of the aperture if the surface brightness profile falls with the inverse of the aperture, which would correspond to an isotropic emission and steady-state coma.

Figure 4 shows the Afρ values as a function of the cometocentric distance calculated for the g, r, i and z bands for the SOAR observations of September 2019. For all filters, there is a steep increase of A$f\rho$ with aperture followed by a gentler decline. The steep increase of $Af\rho$ for smaller aperture radii is the result of the coma's flux being spread out due to the seeing of the observation, while the slow decrease at larger radii may be associated with a non-steady-state dust emission, the effects of solar radiation pressure, possible dust grain fragmentation, or combinations of such mechanisms. The behavior for the z and i bands are similar, but for the g and r band the peak value is shifted to larger apertures and presents a less steep decline. Also, the peak value for the r band reaches a smaller value than for the other filters.

The A$f\rho$ values for the comet C/2017 U7 (PANSTARRS) derived for filters in the SDSS system, are listed in Table 6, with the maximum and the relative aperture radius. Comparing the values obtained from the r-filter in the DES observations in September 2018 with the values from the SOAR data on September 2019, is possible to identify a clear increase in the dust production.

Table 6
Afρ values for comet C 2017 U7 (PANSTARRS), derived for SDSS filter system with reference optical aperture of $\rho = 10^4$ km and centred on the optocentre.

Date	Filter	Afρ (cm) ($\rho = 10^4$ km)	Afρ_{max}	ρ_{max} (km)
2018-09-15	r-band	*1607*	*1662*	14320
2019-09-09	g-band	*2509*	*2555*	12815
2019-09-09	r-band	*2398*	*2331*	12174
2019-09-09	i-band	*2716*	*2724*	10893
2019-09-09	z-band	*2686*	*2691*	10893

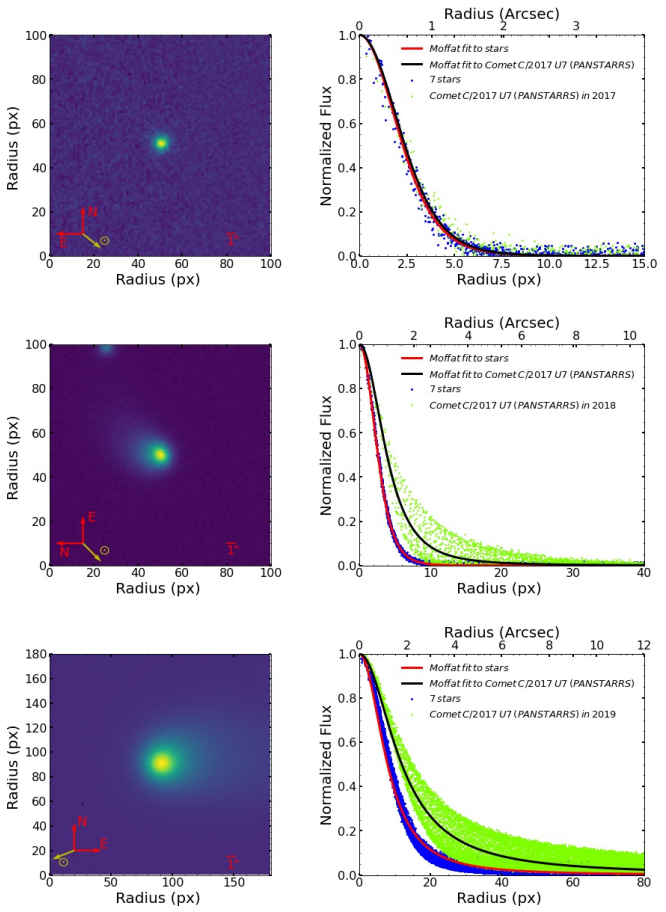

Figure 3: Left: co-added images of C/2017 U7 (PANSTARRS) of October 2017, September 2018, September 2019; right: associated surface brightness profile, with values of the normalized intensity as a function of the distance from de centroid for stars and C/2017 U7 ((PANSTARRS), and Moffat adjustment for stars and C/2017 U7 ((PANSTARRS).

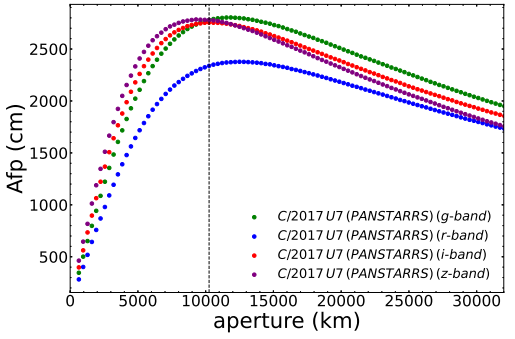

Figure 4: Afρ trend versus cometocentric distance measured for comet C/2017 (PANSTARRS) in g-, r-, i-, z-band filters in SDSS system for observations of September 2019. *The dashed line represents the size from HWHM*

4.2. Colors and Spectral properties

The primary source of information about the spectral behavior of the comet is the low-resolution spectrum obtained on 2018-08-13 and the photometry on the g-,r-,i-,z-bands from the observations on 2019-09-19, which can be used to derive colors as well as a reflectance spectrum. The former set of observations was obtained within an interval of ~ 5 minutes and therefore is not severely affected by temporal variations in the coma. The latter set of $i-z$ and $g-r$ colors of the nucleus were obtained from the DES observations on 2017-10-30 and 2017-11-10.

Figure 5 shows the low-resolution reflectance spectra of the comet along with reflectance spectra obtained from the SDSS magnitudes (Fukugita et al., 1996), using apertures 0.45, 1.95, and 7.2 arcsec. The low-resolution spectrum is peculiar because it presents an absorption band centered around $\sim 0.596\,\mu m$, which is not commonly seen on spectra of comets or asteroids. We used the CANA tool (De Pra et al., 2018) to characterize the center of the band at $\sim 0.596\,\mu m$ and its depth at $7.7 \pm 0.5\%$. The continuum was measured in the regions close to 0.52 and 0.65 μm. The feature is also present in the reflectance spectra obtained from the SDSS colors taken nearly a year after the spectrum when the comet was more active. Because of the presence of this band, we chose to normalize all reflectance spectra to 0.748 μm, which corresponds to the central wavelength of the SDSS i-band filter. Both the overall slope of the spectra and the contrast of the band vary with the aperture used to compute the magnitudes, and the low-resolution spectrum is better matched with an aperture of 1.95 arcsec. Figure 6 presents the color gradient in $g-r$ and $r-i$ as a function of the aperture and clearly shows that there is a marked change in the $r-i$ color that is consistent with the brightness in the $r-$band changing more slowly with the aperture than that of the i-band. This behavior is also consistent with how the $Af\rho$ measurements vary with photometry aperture.

In order to compare C/2017 U7 (PANSTARRS) with other populations, we estimated the object's SDSS nucleus colors from the DES images (when the comet was not displaying a conspicuous coma) and the SDSS spectrophotometric data obtained during the 2019 run (when the object was closer to perihelion and displaying a dust coma) using an aperture of 1.95 arcseconds. In Figure 7, the colors of the comet C/2017 U7 (PANSTARRS) are compared with the distribution of SDSS colors of active comets (Solontoi et al., 2012), Centaurs (Ofek, 2012; Peixinho et al., 2015) and trans-Neptunian objects or TNOs (Terai et al., 2018). It is of note that the colors obtained from (Peixinho et al., 2015) were taken using the $BVRI$ filters, and we transformed to $g-r$, $r-i$ and $i-z$. As seen in the figure, this comet has unusual colors when compared with other comets and also to Centaurs, having some overlap only with TNOs and Centaurs. The main difference between this comet and other objects is due to its $i-z$ and $g-r$ colors, which were also peculiar on the DES observations of 2017-10-30 and 2017-11-10, when there was no discernible coma. This color is

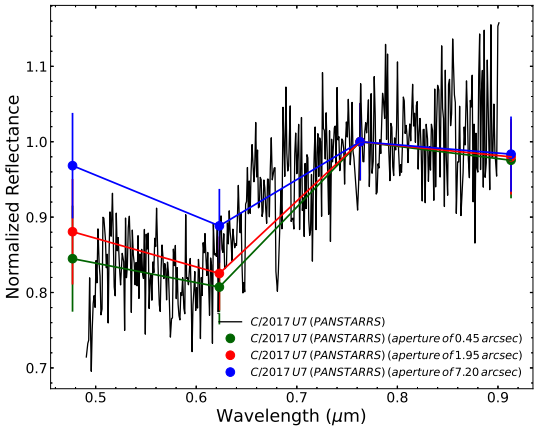

Figure 5: Reflectance spectra of C/2017 U7 (PANSTARRS) from low-resolution spectroscopy and SDSS colors. All spectra were normalized at $0.748\,\mu m$, the spectrum was obtained in August 2018 and the reflectance spectra derived from the SDSS filters were obtained in September 2019.

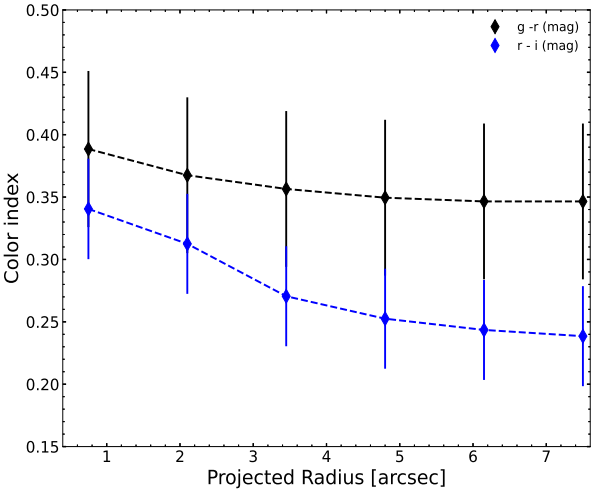

Figure 6: The $g-r$ *and* $r-i$ color as a functions of projected aperture radius of comet C/2017 U7 (PANSTARRS) for observations of September 2019.

the most affected by the presence of the 0.595 μm feature. Figures 8 and 9 compare the SDSS reflectance spectrum of C/2017 U7 (PANSTARRS) with reflectance spectra of comets, TNOs and Centaurs. Again, some similarity is seen only with the spectra of some TNOs and Centaurs.

4.3. Search for spectral analogs

The observed spectrum of a comet in the presence of the coma can differ from the spectrum of the nucleus due to the size distribution of the dust (Rondón-Briceño et al., 2017). However, for the C/2017 U7

(PANSTARRS) the $g-r$ and $i-z$ colors obtained on two different nights shows the object has a blue slope and is similar to what was seen in the DES observations (Figure 7) and this suggests that this band could be a characteristic of the material of the nucleus, but unfortunately, we do not have the r-i color to confirm the observed absorption in the DES data.

In order to identify materials that could produce a similar feature, we conducted a search in the latest release (December 2019) of the RELAB spectral library (RELAB, 2019). A total of 8962 VNIR spectra covering at least the $0.5-0.8$ μm range were inspected for the presence of a feature around 0.595 μm. This sample includes 28 spectra of organic samples, 1840 spectra of meteorite material, 2770 spectra of terrestrial rocks and 4324 spectra of Earth minerals.

The spectra with a feature centered around 0.595 μm were then visually compared with the comet spectrum. This exercise in curve-matching has a limited capacity as a diagnostic of the composition, since the measured spectra are also affected by grain size, sample texture and the experimental geometry. It does however allow one to pinpoint possible candidates. In general, the bands detected in the RELAB spectra were either too shallow or too deep compared with the feature observed in the comet's spectrum, or were present alongside other spectral features not seen in the spectrum of the comet. Figure 10 shows comparisons of the comet's spectrum with some selected RELAB spectra. Some very shallow features were present in several meteorite spectra, but none display a feature that matches the comet's band. This is the case for the samples of the unusual CI Tagish Lake and of the Iron meteorite DRP78007, as well of some mineral and rock samples. On the other hand, the spectrum of the Mesosiderite Barea matches the band, but shows several other features that are not detected in the comet's spectrum. The overall best match is with a spectrum of kerite, an organic kerogen-like material.

5. Summary and Discussion

Comet C/2017 U7 (PANSTARRS), as discussed in section 2, is most likely a dynamically old object from the outer Oort cloud, although the possibility of it being captured from interstellar space cannot be excluded. The propagation of the comet's orbit into the past shows that it may have had at least one but perhaps several perihelion passages in the last *3 Myr*, with the most recent happening around 700,000 years ago, with perihelion distances always close to the present one, $q = 6.417$ au. Our integrations also indicate that this comet has a high probability of being ejected from the solar system after its most recent perihelion passage. Comet C/2017 U7 (PANSTARRS) became active shortly before our first run at SOAR on 2018-08-13, when its distance to the Sun was $r = 6.943$ au, and its $Af\rho$ values increased from $Af\rho = 1662$ cm in 2018-09-15 (at $r = 6.827$ au) to $Af\rho = 2398.15$ cm in 2019-09-19 (at $r = 6.417$ au). Therefore, the activity

started before perihelion and the dust production rates increased as the comet approached its perihelion. The fact that the activity started at $r \approx 7$ au suggests that the main mechanism responsible for the dust production is the transition from amorphous to crystaline water ice, and the measured values of $Af\rho$ are consistent with values reported for other comets that became active at large perihelion distances (Meech et al., 2009). ~~*The absolute magnitude of $H = 10.87$ mag for the nucleus, derived from observations with no indication of activity*~~ *The absolute magnitude of $H = 10.87$ mag as representative of the region for the nucleus, derived from observations with no detected activity*, places comet C/2017 U7 (PANSTARRS) among the largest long-period comets observed so far (Fernández and Sosa, 2012).

C/2017 U7 (PANSTARRS) is also peculiar when compared to most other comets regarding its $g-r$ color: observations of the nucleus have values of $g-r$ smaller than what is observed for comets and centaurs, and the value of this color observed with the presence of the coma is even smaller. Both observations are only compatible with the $g-r$ colors of some TNOs and Centaurs. The low-resolution spectrum and the spectrophotometry in the SDSS system, obtained when the comet was active, show the presence of a large spectral feature similar to an absorption band centered around 0.595 μm, which again is only similar to the spectra obtained from SDSS colors of some TNOs. The fact that the $g-r$ color of the nucleus is also peculiar suggests that this feature is possibly related to the composition of the material in the dust, rather than a product of the size distribution of the dust in the coma, and the lower values of $Af\rho$ obtained in the r filter could be related to the lower albedo of the dust in the corresponding spectral range.

A search for spectral analogs in the RELAB spectral database (RELAB, 2019) shows that a similar feature and overall spectral similarities in the visible can be reproduced by some bireflectance spectra of the organic material kerite. The presence of kerite-like (alongside other kerogen-like materials) on the surface of minor bodies was proposed by Moroz et al. (1992) as a possible explanation for the reddening in the visible spectra of P-, D-type asteroids. Also, kerite has been used as a proxy material for aliphatic-rich hydrocarbons to fit features in the $2.6-3.6$ μm range in the spectra of minor bodies (De Sanctis et al., 2017), and aliphatic-rich hydrocarbons have been previously detected on comets (Raponi et al., 2020). To our knowledge, however, the presence of a spectral feature like the 0.595 μm band observed in C/2017 U7 (PANSTARRS) was never used as a proxy for the presence of aliphatic-rich hydrocarbons on asteroids or comets. Therefore, even if the presence of kerite-like materials is a plausible explanation for the observed 0.595μm feature, it still fails to explain why the visible spectrum of C/2017 U7 (PANSTARRS) is peculiar when compared to the spectra of other comets, which in general present red, featureless spectra in the visible.

A tentative explanation for the unusual spectrum of C/2017 U7 (PANSTARRS) could be proposed considering three points: 1) the dependence of the spectral properties of kerogen-like material on grain size;

2) the low ejection velocity of the assumed dust production mechanism, and 3) the unusually large size of the nucleus. Moroz et al. (1992) remark that the overall redness of the spectra of kerogen-like materials is strongly sensitive to particle size, showing as a example the fact that a asphaltite spectrum with particle in the range $100 - 200$ μm is considerably less red than a spectrum of the same material with particles < 100 μm. The dependence of kerite spectra on particle size as judged by the spectra in the RELAB database is not so clear, however. Out of the nine related spectra in the database, the only one with particles in the range $100 - 200$ μm does show both a clear band in the 0.595 μm and a neutral spectral inclination in the visible. However, the reddest spectra have particles < 200 μm, while an additional spectrum with this particle range presents an intermediate spectral inclination similar to the spectra obtained with particles < 100 μm, among which it is the best match spectrum shown in Figure 10. This inconsistency however can be attributed to the processes involved in sample preparation, since while repeated sieving can in principle effectively limit particle sizes, the contribution of the smaller particles of samples without a defined lower limit depends on how each sample was grinded. The available samples are consistent with the interpretation that the reddening of the kerite spectra that masks the presence of the 0.595 μm band is caused by the predominance of particles < 100 μm. If that is so, the peculiar spectra and colors of C/2017 U7 (PANSTARRS) could be explained if we assume that both its surface and its coma have a higher contribution of larger organic-rich particles than most comets. This unusual particle size distribution may be a consequence of the fact that dust particles released due to the transition of amorphous to crystalline water ice tend to have low ejection velocities, with somewhat lower velocities for larger particles (Meech et al., 2009), and therefore the relatively larger escape velocity from the nucleus could produce a particle size segregation in the coma, with larger particles spreading at a slower pace and thus being more densely packed than smaller particles. Also, in this scenario the larger particles would be more likely to return to or to remain close to the surface, so this surface particle size segregation resulting from previous perihelion passages could also explain the unusual colors of the nucleus.

This hypothesis could be tested quantitatively with a model like the one presented by Rondón-Briceño et al. (2017), but for that it would be necessary to obtain a consistent set of optical constants for kerite, and a larger time coverage of the expansion of the coma would also be desirable. Work to this end is currently under way. If this mechanism proves to be viable, it could also provide some insight on the spectral similarities observed with respect to the TNO population. It is worth noticing that C/2017 U7 (PANSTARRS) has a probable solar system origin, the unique spectral properties in addition to the non-null possibility of it being captured from interstellar space, might suggest that this latter scenario could also be plausible.

Acknowledgments

M. E. Santana acknowledges funding through a CAPES PhD fellowship. J. M. Carvano ackowledges funding through a CNPq fellowship. M. De Prá acknowledges funding through the Preeminent Post-Doctoral Program (P3) at the University of Central Florida.

Based on observations obtained at the Southern Astrophysical Research (SOAR) telescope, which is a joint project of the Ministério da Ciência, Tecnologia e Inovações (MCTI/LNA) do Brasil, the US National Science Foundation's NOIRLab, the University of North Carolina at Chapel Hill (UNC), and Michigan State University (MSU).

This project used public archival data from the Dark Energy Survey (DES). Funding for the DES Projects has been provided by the U.S. Department of Energy, the U.S. National Science Foundation, the Ministry of Science and Education of Spain, the Science and Technology FacilitiesCouncil of the United Kingdom, the Higher Education Funding Council for England, the National Center for Supercomputing Applications at the University of Illinois at Urbana-Champaign, the Kavli Institute of Cosmological Physics at the University of Chicago, the Center for Cosmology and Astro-Particle Physics at the Ohio State University, the Mitchell Institute for Fundamental Physics and Astronomy at Texas A&M University, Financiadora de Estudos e Projetos, Fundação Carlos Chagas Filho de Amparo à Pesquisa do Estado do Rio de Janeiro, Conselho Nacional de Desenvolvimento Científico e Tecnológico and the Ministério da Ciência, Tecnologia e Inovação, the Deutsche Forschungsgemeinschaft, and the Collaborating Institutions in the Dark Energy Survey. The Collaborating Institutions are Argonne National Laboratory, the University of California at Santa Cruz, the University of Cambridge, Centro de Investigaciones Energéticas, Medioambientales y Tecnológicas-Madrid, the University of Chicago, University College London, the DES-Brazil Consortium, the University of Edinburgh, the Eidgenössische Technische Hochschule (ETH) Zürich, Fermi National Accelerator Laboratory, the University of Illinois at Urbana-Champaign, the Institut de Ciències de l'Espai (IEEC/CSIC), the Institut de Física d'Altes Energies, Lawrence Berkeley National Laboratory, the Ludwig-Maximilians Universität München and the associated Excellence Cluster Universe, the University of Michigan, the National Optical Astronomy Observatory, the University of Nottingham, The Ohio State University, the OzDES Membership Consortium, the University of Pennsylvania, the University of Portsmouth, SLAC National Accelerator Laboratory, Stanford University, the University of Sussex, and Texas A&M University. Based in part on observations at Cerro Tololo Inter-American Observatory, National Optical Astronomy Observatory, which is operated by the Association of Universities for Research in Astronomy (AURA) under a cooperative agreement with the National Science Foundation.

CdlFM and RdlFM thank S. J. Aarseth for providing one of the codes used in this research and A. I.

Gómez de Castro for providing access to computing facilities. Part of the calculations and the data analysis were completed on the Brigit HPC server of the 'Universidad Complutense de Madrid' (UCM), and we thank S. Cano Alsúa for his help during this stage. This work was partially supported by the Spanish 'Ministerio de Economía y Competitividad' (MINECO) under grant ESP2017-87813-R.

CRediT authorship contribution statement

M. Evangelista-Santana: Data Reduction, Data Analysis, Writing. **J. M. Carvano:** Co-ordination, Methodology, Data Analysis, Writing. **M. De Prá:** Observing time proposal preparation, Observation, Data Reduction, Data Analysis, Writing . **R. de la Fuente Marcos:** Dynamical analysis. **C. Schambeau:** Cometary activity analysis, Observations, Writing. **J. Licandro:** Cometary activity analysis, Observations. **C. de la Fuente Marcos:** Dynamical analysis. **A. C. Souza-Feliciano:** Observations. **N. Pinilla-Alonso:** Observations.

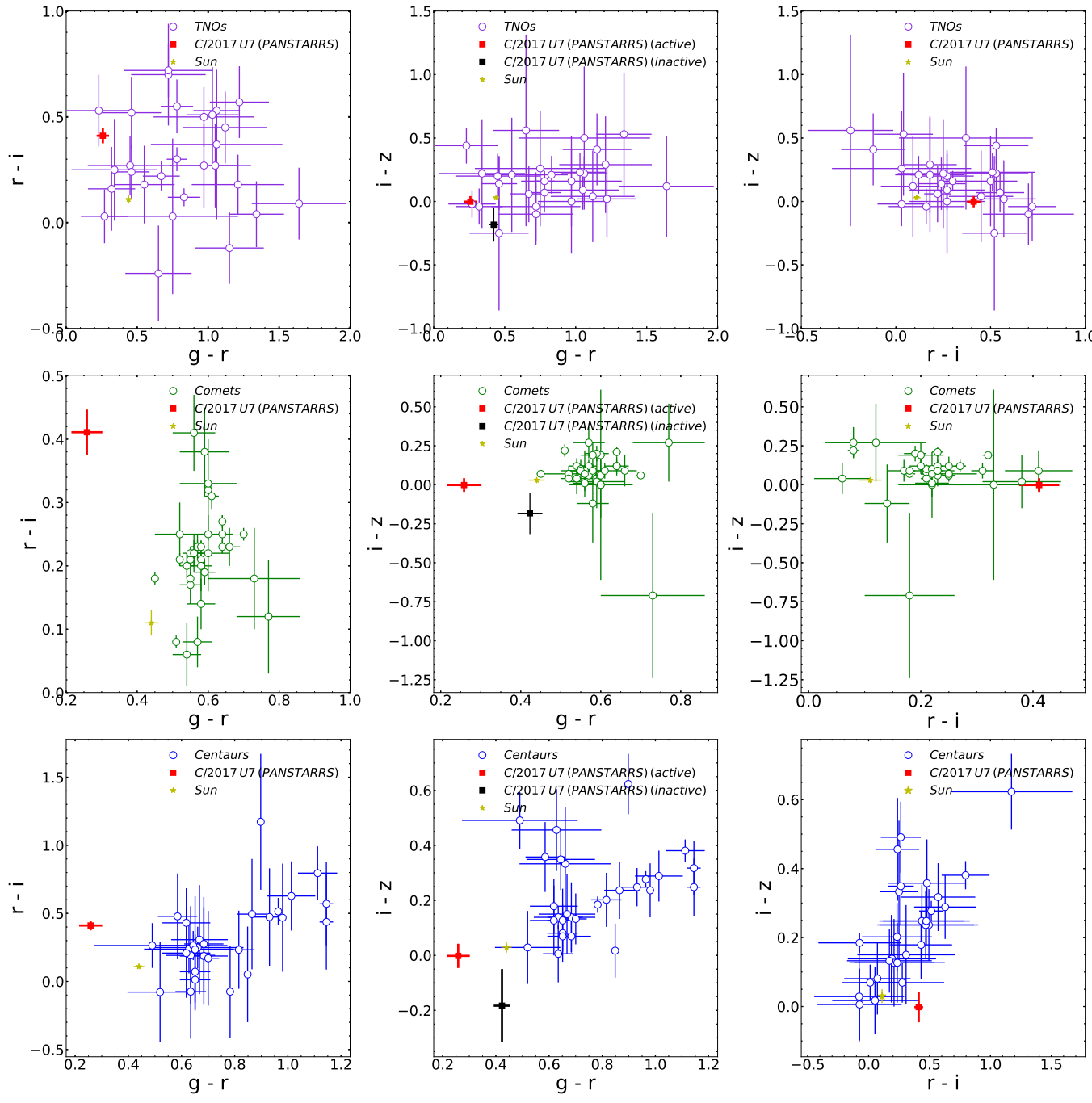

Figure 7: Color-color diagrams of the colors for different minor bodies populations showing the color of C/2017 U7 (PANSTARRS) inative (obtained from the DES) and active (obtained from the SOAR). The TNOs colors are from Terai et al. (2018); the comets colors are from Solontoi et al. (2012) and the Centaurs colors are from (Ofek, 2012; Peixinho et al., 2015).

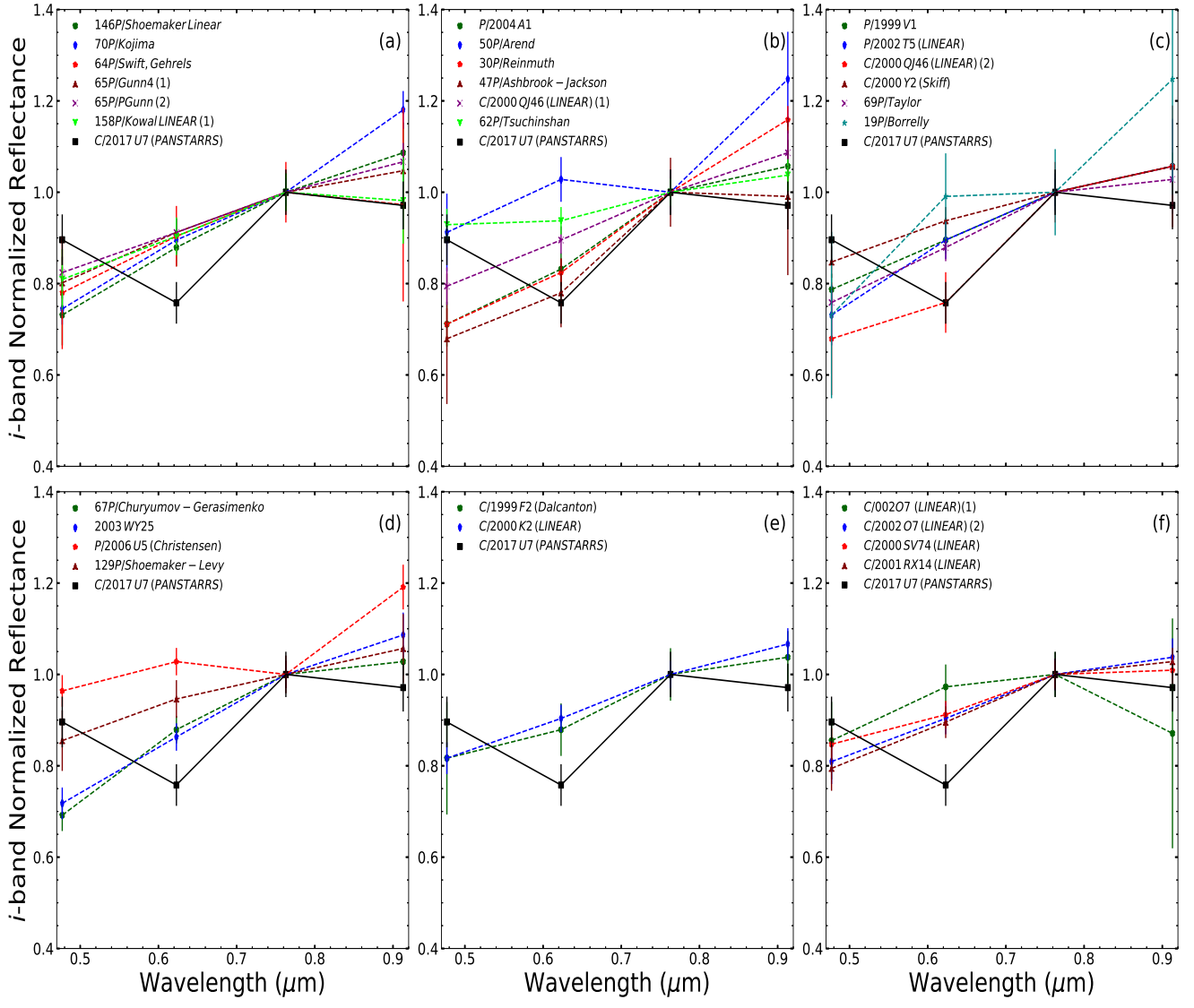

Figure 8: Normalized reflectance spectra for comparing C/2017 (PANSTARRS) (aperture 1.95 arcsec) with different types of comets. In order to compare, we show: (a), (b), (c), (d) Jupiter Family Comets; (e) comets with no defined group and (f) hyperbolic comets. The Comets are from Solontoi et al. (2012).

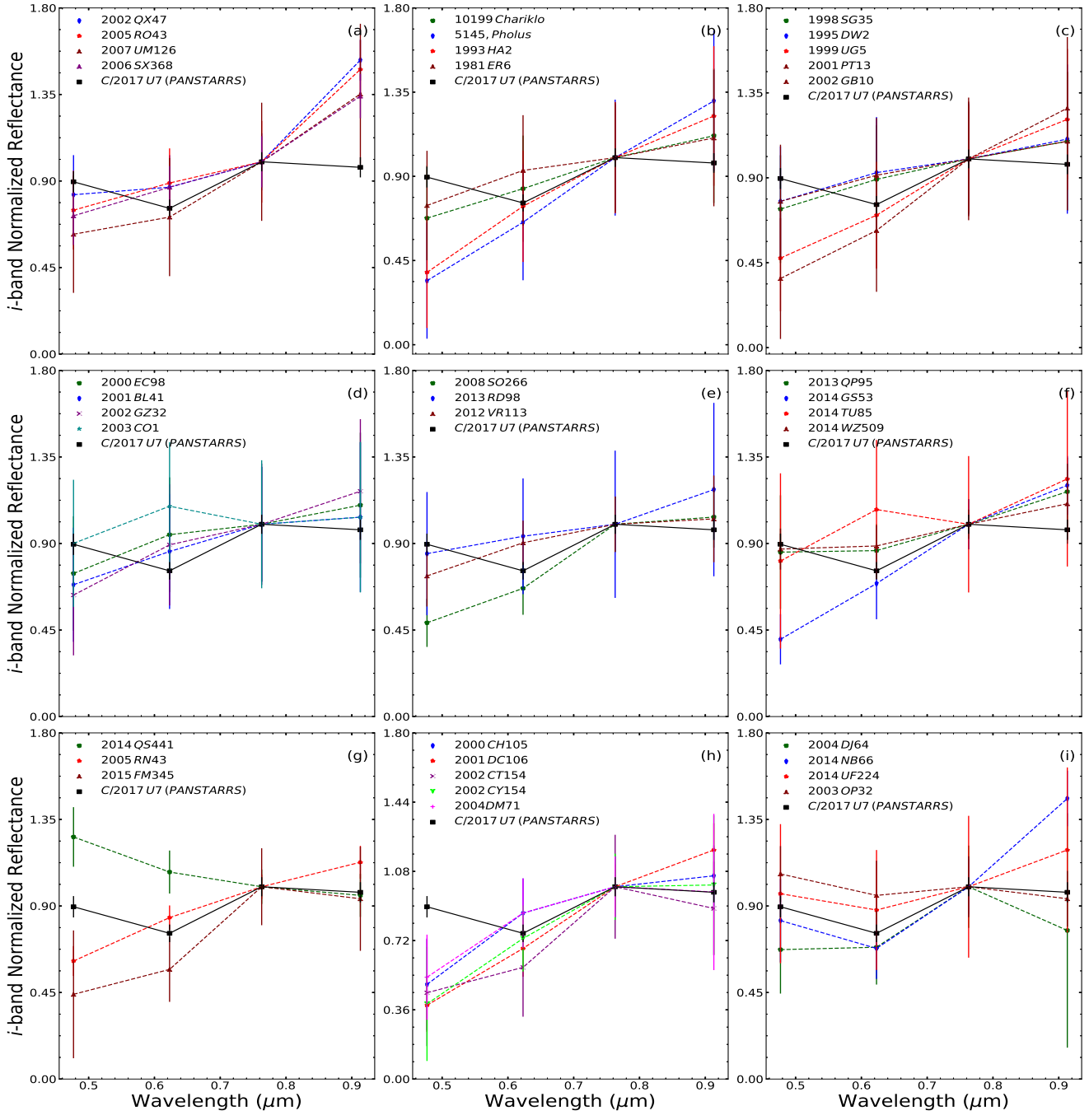

Figure 9: Normalized reflectance spectra of Centaurs and TNOs populations in comparison with comet C/2017 (PANSTARRS). (a), (b), (c), (d) and (e) Centaurs ; (f), (g), (h) and (i) TNOs. The Centaurs are from Ofek (2012); Peixinho et al. (2015); the TNOs are from Terai et al. (2018).

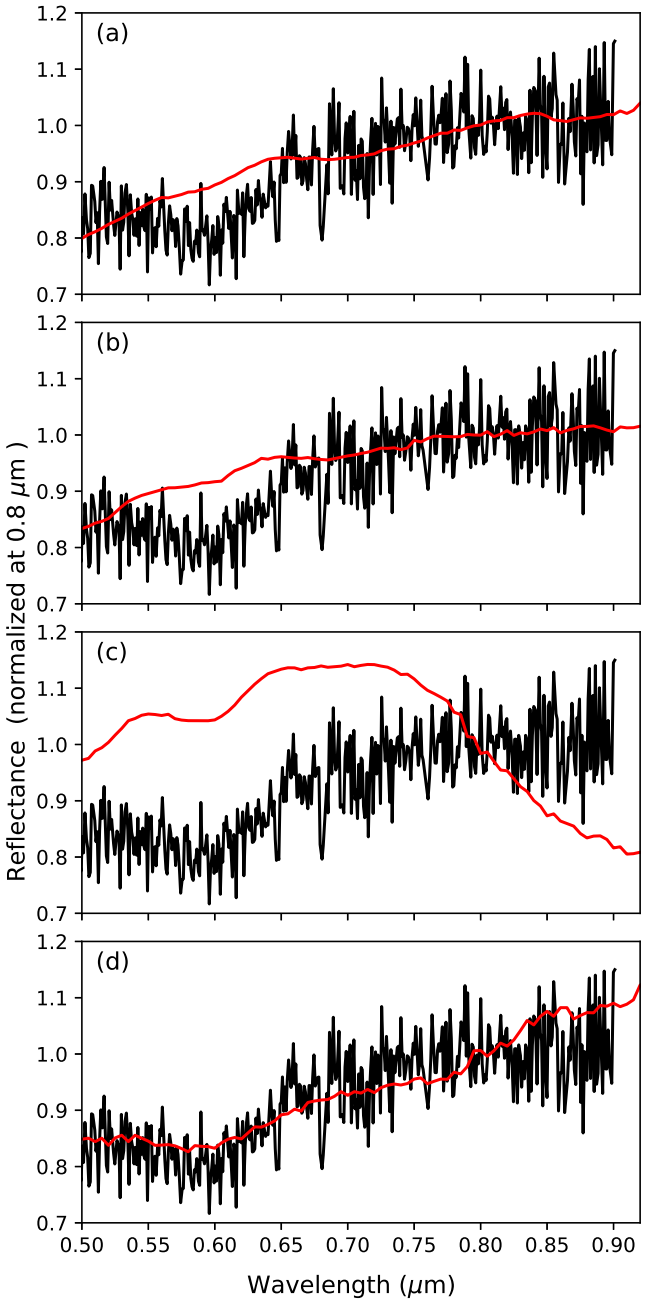

Figure 10: Comparison of the reflectance spectra of C/2017 U7 (PANSTARRS) *in black* with selected RELAB spectra *in red* (spectral file name between parentheses): (a) unusual CI Tagish Lake (C1MT237B); (b) Iron Meteorite DRP78007 (CFMB47); (c) Mesosiderite Barea (C1MB33); (d) Kerite sample #13 (CAMS22).

References

Aarseth, S.J., 2003. Gravitational N-Body Simulations.

A'Hearn, M.F., Schleicher, D.G., Millis, R.L., Feldman, P.D., Thompson, D.T., 1984. Comet Bowell 1980b. AJ 89, 579–591. doi:10.1086/113552.

Alvarez-Candal, A., Pinilla-Alonso, N., Ortiz, J.L., Duffard, R., Morales, N., Santos-Sanz, P., Thirouin, A., Silva, J.S., 2016. Absolute magnitudes and phase coefficients of trans-Neptunian objects. A&A 586, A155. doi:10.1051/0004-6361/201527161, arXiv:1511.09401.

Bauer, J.M., Grav, T., Fernández, Y.R., Mainzer, A.K., Kramer, E.A., Masiero, J.R., Spahr, T., Nugent, C.R., Stevenson, R.A., Meech, K.J., Cutri, R.M., Lisse, C.M., Walker, R., Dailey, J.W., Rosser, J., Krings, P., Ruecker, K., Wright, E.L., NEOWISE Team, 2017. Debiasing the NEOWISE Cryogenic Mission Comet Populations. AJ 154, 53. doi:10.3847/1538-3881/aa72df.

Branham, R. L., J., 2013. New Orbits for Comets C/1960 M1 (Humason), C/1980 E1 (Bowell), and Musings on Extrasolar Comets. Rev. Mexicana Astron. Astrofis. 49, 111–116.

Bressi, T.H., Camilleri, P., Oey, J., Gilmore, A.C., Kilmartin, P.M., Meech, K.J., Kleyna, J., Wipper, C., Micheli, M., Linder, T., Holmes, R., Miller, P., Gomez, E., Miles, R., Buzzi, L., Foglia, S., Bulger, J., Lowe, T., Schultz, A., Willman, M., Chambers, K., Chastel, S., Denneau, L., Flewelling, H., Huber, M., Lilly, E., Magnier, E., Wainscoat, R., Waters, C., Weryk, R., Abreu, D., Koschny, D., Knoefel, A., Busch, M., Schwab, E., Mattiazzo, M., Sato, H., Urbanik, M., Hale, A., Heinze, A., Weiland, H., Tonry, J., Fitzsimmons, A., Young, D., Stalder, B., Robinson, B., Erasmus, N., Armstrong, J.D., Teagarden, Z.N., Ryden, S.W., Moss, S.R., Kocsis, A., Nagy Melykuti, A., Sarneczky, K., Zalezsak, T., 2020. COMET C/2017 U7 (PANSTARRS). Minor Planet Electronic Circulars 2020-F58.

Bressi, T.H., Meech, K.J., Kleyna, J., Wipper, C., Micheli, M., Linder, T., Holmes, R., Miller, P., Gomez, E., Miles, R., Buzzi, L., Foglia, S., Bulger, J., Lowe, T., Schultz, A., Willman, M., Chambers, K., Chastel, S., Denneau, L., Flewelling, H., Huber, M., Lilly, E., Magnier, E., Wainscoat, R., Waters, C., Weryk, R., Abreu, D., Koschny, D., Knoefel, A., Busch, M., Schwab, E., Sato, H., Armstrong, J.D., Teagarden, Z.N., Ryden, S.W., Moss, S.R., Williams, G.V., 2018. A/2017 U7. Minor Planet Electronic Circulars 2018-E17.

Buffoni, L., Scardia, M., Manara, A., 1982. The orbital evolution of comet Bowell (1980b). Moon and Planets 26, 311–315. doi:10.1007/BF00928013.

Chebotarev, G.A., 1965. On the Dynamical Limites of the Solar System. Soviet Ast. 8, 787.

de la Fuente Marcos, C., de la Fuente Marcos, R., 2012. On the dynamical evolution of 2002 VE_{68}. MNRAS 427, 728–739. doi:10.1111/j.1365-2966.2012.21936.x, arXiv:1208.4444.

de la Fuente Marcos, C., de la Fuente Marcos, R., 2015. Asteroid 2015 DB_{216}: a recurring co-orbital companion to Uranus. MNRAS 453, 1288–1296. doi:10.1093/mnras/stv1725, arXiv:1507.07449.

de la Fuente Marcos, C., de la Fuente Marcos, R., 2019. Comet C/2018 V1 (Machholz-Fujikawa-Iwamoto): dislodged from the Oort Cloud or coming from interstellar space? MNRAS 489, 951–961. doi:10.1093/mnras/stz2229, arXiv:1908.02666.

de la Fuente Marcos, C., de la Fuente Marcos, R., Aarseth, S.J., 2018. Where the Solar system meets the solar neighbourhood: patterns in the distribution of radiants of observed hyperbolic minor bodies. MNRAS 476, L1–L5. doi:10.1093/mnrasl/sly019, arXiv:1802.00778.

de la Fuente Marcos, C., de la Fuente Marcos, R., Licandro, J., Serra-Ricart, M., Cabrera-Lavers, A., 2019. Ordinary Oort Cloud Comets: An Update on the Past and Future Orbital Evolution of C/2018 F4 (PANSTARRS). Research Notes of the

American Astronomical Society 3, 143. doi:10.3847/2515-5172/ab4888.

de la Fuente Marcos, R., de la Fuente Marcos, C., 2018. Comet C/2017 K2 (PANSTARRS): Dynamically Old or New? Research Notes of the American Astronomical Society 2, 10. doi:10.3847/2515-5172/aabf8f, arXiv:1804.07292.

de León, J., Licandro, J., de la Fuente Marcos, C., de la Fuente Marcos, R., Lara, L.M., Moreno, F., Pinilla-Alonso, N., Serra-Ricart, M., De Prá, M., Tozzi, G.P., Souza-Feliciano, A.C., Popescu, M., Scarpa, R., Font Serra, J., Geier, S., Lorenzi, V., Harutyunyan, A., Cabrera-Lavers, A., 2020. Visible and near-infrared observations of interstellar comet 2I/Borisov with the 10.4-m GTC and the 3.6-m TNG telescopes. MNRAS 495, 2053–2062. doi:10.1093/mnras/staa1190, arXiv:2005.00786.

De Pra, M.N., Carvano, J., Morate, D., Pinilla-Alonso, N., Licandro, J., 2018. CANA: A Python package for the analysis of hydration in asteroid spectroscopic and spectrophotometric data, in: AAS/Division for Planetary Sciences Meeting Abstracts #50, p. 315.02.

De Prá, M.N., Licandro, J., Pinilla-Alonso, N., Lorenzi, V., Rondón, E., Carvano, J., Morate, D., De León, J., 2020. The spectroscopic properties of the Lixiaohua family, cradle of Main Belt Comets. Icarus 338, 113473. doi:10.1016/j.icarus.2019.113473.

De Sanctis, M.C., Ammannito, E., McSween, H.Y., Raponi, A., Marchi, S., Capaccioni, F., Capria, M.T., Carrozzo, F.G., Ciarniello, M., Fonte, S., Formisano, M., Frigeri, A., Giardino, M., Longobardo, A., Magni, G., McFadden, L.A., Palomba, E., Pieters, C.M., Tosi, F., Zambon, F., Raymond, C.A., Russell, C.T., 2017. Localized aliphatic organic material on the surface of Ceres. Science 355, 719–722. doi:10.1126/science.aaj2305.

Denneau, L., Jedicke, R., Grav, T., Granvik, M., Kubica, J., Milani, A., Vereš, P., Wainscoat, R., Chang, D., Pierfederici, F., Kaiser, N., Chambers, K.C., Heasley, J.N., Magnier, E.A., Price, P.A., Myers, J., Kleyna, J., Hsieh, H., Farnocchia, D., Waters, C., Sweeney, W.H., Green, D., Bolin, B., Burgett, W.S., Morgan, J.S., Tonry, J.L., Hodapp, K.W., Chastel, S., Chesley, S., Fitzsimmons, A., Holman, M., Spahr, T., Tholen, D., Williams, G.V., Abe, S., Armstrong, J.D., Bressi, T.H., Holmes, R., Lister, T., McMillan, R.S., Micheli, M., Ryan, E.V., Ryan, W.H., Scotti, J.V., 2013. The Pan-STARRS Moving Object Processing System. PASP 125, 357. doi:10.1086/670337, arXiv:1302.7281.

Everhart, E., 1982. Evolution of long- and short-period orbits, in: Wilkening, L.L. (Ed.), IAU Colloq. 61: Comet Discoveries, Statistics, and Observational Selection, pp. 659–664.

Fernández, J.A., Gallardo, T., Brunini, A., 2004. The scattered disk population as a source of Oort cloud comets: evaluation of its current and past role in populating the Oort cloud. Icarus 172, 372–381. doi:10.1016/j.icarus.2004.07.023.

Fernández, J.A., Sosa, A., 2012. Magnitude and size distribution of long-period comets in Earth-crossing or approaching orbits. MNRAS 423, 1674–1690. doi:10.1111/j.1365-2966.2012.20989.x, arXiv:1204.2285.

Fernández, Y.R., Kelley, M.S., Lamy, P.L., Toth, I., Groussin, O., Lisse, C.M., A'Hearn, M.F., Bauer, J.M., Campins, H., Fitzsimmons, A., Licandro, J., Lowry, S.C., Meech, K.J., Pittichová, J., Reach, W.T., Snodgrass, C., Weaver, H.A., 2013. Thermal properties, sizes, and size distribution of Jupiter-family cometary nuclei. Icarus 226, 1138–1170. doi:10.1016/j.icarus.2013.07.021, arXiv:1307.6191.

Flaugher, B., Diehl, H.T., Honscheid, K., Abbott, T.M.C., Alvarez, O., Angstadt, R., Annis, J.T., Antonik, M., Ballester, O., Beaufore, L., Bernstein, G.M., Bernstein, R.A., Bigelow, B., Bonati, M., Boprie, D., Brooks, D., Buckley-Geer, E.J., Campa, J., Cardiel-Sas, L., Castand er, F.J., Castilla, J., Cease, H., Cela-Ruiz, J.M., Chappa, S., Chi, E., Cooper, C., da Costa, L.N., Dede, E., Derylo, G., DePoy, D.L., de Vicente, J., Doel, P., Drlica-Wagner, A., Eiting, J., Elliott, A.E., Emes, J., Estrada, J., Fausti Neto, A., Finley, D.A., Flores, R., Frieman, J., Gerdes, D., Gladders, M.D., Gregory, B., Gutierrez, G.R., Hao,

J., Holland, S.E., Holm, S., Huffman, D., Jackson, C., James, D.J., Jonas, M., Karcher, A., Karliner, I., Kent, S., Kessler, R., Kozlovsky, M., Kron, R.G., Kubik, D., Kuehn, K., Kuhlmann, S., Kuk, K., Lahav, O., Lathrop, A., Lee, J., Levi, M.E., Lewis, P., Li, T.S., Mand richenko, I., Marshall, J.L., Martinez, G., Merritt, K.W., Miquel, R., Muñoz, F., Neilsen, E.H., Nichol, R.C., Nord, B., Ogando, R., Olsen, J., Palaio, N., Patton, K., Peoples, J., Plazas, A.A., Rauch, J., Reil, K., Rheault, J.P., Roe, N.A., Rogers, H., Roodman, A., Sanchez, E., Scarpine, V., Schindler, R.H., Schmidt, R., Schmitt, R., Schubnell, M., Schultz, K., Schurter, P., Scott, L., Serrano, S., Shaw, T.M., Smith, R.C., Soares-Santos, M., Stefanik, A., Stuermer, W., Suchyta, E., Sypniewski, A., Tarle, G., Thaler, J., Tighe, R., Tran, C., Tucker, D., Walker, A.R., Wang, G., Watson, M., Weaverdyck, C., Wester, W., Woods, R., Yanny, B., DES Collaboration, 2015. The Dark Energy Camera. AJ 150, 150. doi:10.1088/0004-6256/150/5/150, arXiv:1504.02900.

Fukugita, M., Ichikawa, T., Gunn, J.E., Doi, M., Shimasaku, K., Schneider, D.P., 1996. The Sloan Digital Sky Survey Photometric System. AJ 111, 1748. doi:10.1086/117915.

Giorgini, J.D., 2015. Status of the JPL Horizons Ephemeris System, in: IAU General Assembly, p. 2256293.

Hainaut, O.R., Meech, K.J., Micheli, M., Belton, M.S.J., 2018. Rendezvous with 'Oumuamua. The Messenger 173, 13–16. doi:10.18727/0722-6691/5092.

Howell, S.B., 1990. CCD growth curves: application to faint and crowded point sources., in: Jacoby, G.H. (Ed.), CCDs in astronomy, pp. 312–318.

Hui, M.T., 2018. Two Hyperbolic Baldheads in the Solar System: 2017 U7 and 2018 C2. AJ 156, 73. doi:10.3847/1538-3881/aacdf3, arXiv:1806.06904.

Jewitt, D., 2015. Color Systematics of Comets and Related Bodies. AJ 150, 201. doi:10.1088/0004-6256/150/6/201, arXiv:1510.07069.

Jurić, M., Ivezić, Ž., Lupton, R.H., Quinn, T., Tabachnik, S., Fan, X., Gunn, J.E., Hennessy, G.S., Knapp, G.R., Munn, J.A., Pier, J.R., Rockosi, C.M., Schneider, D.P., Brinkmann, J., Csabai, I., Fukugita, M., 2002. Comparison of Positions and Magnitudes of Asteroids Observed in the Sloan Digital Sky Survey with Those Predicted for Known Asteroids. AJ 124, 1776–1787. doi:10.1086/341950, arXiv:astro-ph/0202468.

Kaiser, N., 2004. Pan-STARRS: a wide-field optical survey telescope array, in: Oschmann, Jacobus M., J. (Ed.), Ground-based Telescopes, pp. 11–22. doi:10.1117/12.552472.

Keller, S.C., Schmidt, B.P., Bessell, M.S., Conroy, P.G., Francis, P., Granlund, A., Kowald, E., Oates, A.P., Martin-Jones, T., Preston, T., Tisserand , P., Vaccarella, A., Waterson, M.F., 2007. The SkyMapper Telescope and The Southern Sky Survey. PASA 24, 1–12. doi:10.1071/AS07001, arXiv:astro-ph/0702511.

Królikowska, M., Dybczyński, P.A., 2017. Oort spike comets with large perihelion distances. MNRAS 472, 4634–4658. doi:10.1093/mnras/stx2157, arXiv:1708.09248.

Królikowska, M., Dybczyński, P.A., 2018. Dynamical evolution of C/2017 K2 PANSTARRS. A&A 615, A170. doi:10.1051/0004-6361/201832917, arXiv:1802.10380.

Licandro, J., de la Fuente Marcos, C., de la Fuente Marcos, R., de León, J., Serra-Ricart, M., Cabrera-Lavers, A., 2019. Spectroscopic and dynamical properties of comet C/2018 F4, likely a true average former member of the Oort cloud. A&A 625, A133. doi:10.1051/0004-6361/201834902, arXiv:1903.10838.

Licandro, J., Serra-Ricart, M., Oscoz, A., Casas, R., Osip, D., 2000. The Effect of Seeing Variations in Time-Series CCD Inner Coma Photometry of Comets: A New Correction Method. AJ 119, 3133–3144. doi:10.1086/301406.

Luu, J.X., Jewitt, D.C., 1992. High resolution surface brightness profiles of near-earth asteroids. Icarus 97, 276–287. doi:10.1016/0019-1035(92)90134-S.

Makino, J., 1991. Optimal Order and Time-Step Criterion for Aarseth-Type N-Body Integrators. ApJ 369, 200. doi:10.1086/169751.

Martino, S., Tancredi, G., Monteiro, F., Lazzaro, D., Rodrigues, T., 2019. Monitoring of Asteroids in Cometary Orbits and Active Asteroids. Planet. Space Sci. 166, 135–148. doi:10.1016/j.pss.2018.09.001.

Meech, K.J., Pittichová, J., Bar-Nun, A., Notesco, G., Laufer, D., Hainaut, O.R., Lowry, S.C., Yeomans, D.K., Pitts, M., 2009. Activity of comets at large heliocentric distances pre-perihelion. Icarus 201, 719–739. doi:10.1016/j.icarus.2008.12.045.

Meech, K.J., Yang, B., Kleyna, J., Hainaut, O.R., Berdyugina, S., Keane, J.V., Micheli, M., Morbidelli, A., Wainscoat, R.J., 2016. Inner solar system material discovered in the Oort cloud. Science Advances 2, e1600038. doi:10.1126/sciadv.1600038.

Moroz, L.V., Pieters, C.M., Akhmanova, M.V., 1992. Why the Surfaces of Outer Belt Asteroids are Dark and Red?, in: Lunar and Planetary Science Conference, p. 931.

Ofek, E.O., 2012. Sloan Digital Sky Survey Observations of Kuiper Belt Objects: Colors and Variability. ApJ 749, 10. doi:10.1088/0004-637X/749/1/10, arXiv:1202.1538.

Oort, J.H., 1950. The structure of the cloud of comets surrounding the Solar System and a hypothesis concerning its origin. Bull. Astron. Inst. Netherlands 11, 91–110.

Park, R.S., Folkner, W.M., Williams, J.G., Boggs, D.H., 2021. The JPL Planetary and Lunar Ephemerides DE440 and DE441. AJ 161, 105. doi:10.3847/1538-3881/abd414.

Peixinho, N., Delsanti, A., Doressoundiram, A., 2015. Reanalyzing the visible colors of Centaurs and KBOs: what is there and what we might be missing. A&A 577, A35. doi:10.1051/0004-6361/201425436, arXiv:1502.04145.

Portegies Zwart, S., Torres, S., Cai, M.X., Brown, A.G.A., 2021. Oort cloud Ecology. II. the chronology of the formation of the Oort cloud. A&A 652, A144. doi:10.1051/0004-6361/202040096, arXiv:2105.12816.

Raponi, A., Ciarniello, M., Capaccioni, F., Mennella, V., Filacchione, G., Vinogradoff, V., Poch, O., Beck, P., Quirico, E., De Sanctis, M.C., Moroz, L., Kappel, D., Erard, S., Bockelée-Morvan, D., Longobardo, A., Tosi, F., Palomba, E., Combe, J.P., Rousseau, B., Arnold, G., Carlson, R.W., Pommerol, A., Pilorget, C., Fornasier, S., Bellucci, G., Barucci, A., Mancarella, F., Formisan, M., Rinaldi, G., Istiqomah, I., Leyrat, C., 2020. Infrared detection of aliphatic organics on a cometary nucleus. arXiv e-prints , arXiv:2009.14476arXiv:2009.14476.

RELAB, 2019. RELAB spectral database. http://www.planetary.brown.edu/relabdocs/relab_disclaimer.htm. Version: 2019-12-31.

Rondón-Briceño, E., Carvano, J.M., Lorenz-Martins, S., 2017. A study of the effects of faint dust comae on the spectra of asteroids. MNRAS 468, 1556–1566. doi:10.1093/mnras/stx536.

Solontoi, M., Ivezić, Ž., Jurić, M., Becker, A.C., Jones, L., West, A.A., Kent, S., Lupton, R.H., Claire, M., Knapp, G.R., Quinn, T., Gunn, J.E., Schneider, D.P., 2012. Ensemble properties of comets in the Sloan Digital Sky Survey. Icarus 218, 571–584. doi:10.1016/j.icarus.2011.10.008, arXiv:1202.3999.

Stern, S.A., Weissman, P.R., 2001. Rapid collisional evolution of comets during the formation of the Oort cloud. Nature 409, 589–591.

Terai, T., Yoshida, F., Ohtsuki, K., Lykawka, P.S., Takato, N., Higuchi, A., Ito, T., Komiyama, Y., Miyazaki, S., Wang, S.Y., 2018. Multi-band photometry of trans-Neptunian objects in the Subaru Hyper Suprime-Cam survey. PASJ 70, S40.

doi:10.1093/pasj/psx105, arXiv:1704.05941.

Weissman, P.R., 1982. Dynamical history of the Oort Cloud, in: Wilkening, L.L. (Ed.), IAU Colloq. 61: Comet Discoveries, Statistics, and Observational Selection, pp. 637–658.